

Transport of explosive chemicals from the landmine burial in granular soils

Transporte de explosivos químicos provenientes del enterramiento de minas en suelos granulares

Juan Pablo Gutiérrez^{1}, Ingrid Padilla², Luis Dario Sánchez¹*

¹Faculty of Engineering, Universidad del Valle, Cinara Institute, Calle 13 N.º 100-00, Cali, Colombia

²Department of Civil Engineering and Surveying, University of Puerto Rico, Carretera 108 Km. 1.0, Mayagüez, Puerto Rico

(Recibido el 10 de junio de 2009. Aceptado el 8 de septiembre de 2010)

Abstract

The transport of explosive-related chemicals (ERCs) in soils was studied during water infiltration and evaporation processes as a function of soil water content and temperature. The experiments were conducted in two 100 cm uniform cylindrical columns packed with homogeneous sand, and instrumented with air and water pressure sensors and sampling ports to monitor hydraulic conditions and ERCs concentration profiles in soil. TNT and DNT crystals were placed in a porous membrane and buried as a point source near the surface of the soil. Spatial and temporal concentration distributions of conservative solutes were used to evaluate transport behavior of TNT and DNT in soils. Velocity variations and comparison with the numerical model HYDRUS-2D indicate the presence of preferential flow paths. Water content and movement near TNT and DNT buried source highly influence their transport in soils and near soil-atmospheric surfaces. The formation of preferential flow paths are attributed to disturbances of soil properties by burial of ERC sources and water content heterogeneities. By the analysis of velocity variations, disturbances near the buried source resulted in hydraulic heterogeneities and preferential flow near the source, which influence their transport away from the source. Preferential flow causes faster movement and greater dispersion of the solutes during infiltration periods, and influences the rate of mixing in the system.

----- **Keywords:** Advection, evaporation, explosive related chemicals, infiltration, landmine burial, preferential flow paths

* Autor de correspondencia: teléfono: 57 + 2 + 339 23 45, fax: 57 + 2 + 339 32 89, correo electrónico: juanpagu@univalle.edu.co. (J. Gutiérrez)

Resumen

El transporte de compuestos químicos relacionados con explosivos (ERCs) en suelos se estudió durante procesos de infiltración y evaporación de agua como función del contenido de agua del suelo y la temperatura. Los experimentos fueron desarrollados en dos columnas cilíndricas uniformes de 100 cm de longitud empacadas con arena homogénea, equipada con sensores de presión de aire y de agua y puntos de muestreo para monitorear las condiciones hidráulicas y los perfiles de concentraciones de ERCs en el suelo. Los cristales de TNT y DNT fueron localizados en una membrana porosa y se enterraron como fuente puntual cerca de la superficie del suelo. Las distribuciones espaciales y temporales de la concentración de solutos conservadores fueron utilizadas para evaluar el comportamiento del transporte de TNT y del DNT en suelo granular. Las variaciones de velocidad y la comparación con los resultados de la simulación numérica usando el modelo HYDRUS-2D indica la presencia de flujos preferenciales. El contenido de agua y el movimiento de agua alrededor de la fuente enterrada de TNT y DNT influencia altamente su transporte en suelos granulares y cerca de la superficie que interactúa con la atmósfera. La formación de caminos preferenciales son atribuidos a la alteración de las propiedades del suelo debido al enterramiento de las fuentes de ERC y a las heterogeneidades en el contenido de agua. Las alteraciones alrededor de la fuente enterrada que conlleva a heterogeneidades hidráulicas, influye en el transporte cerca a la fuente. El flujo preferencial produce un movimiento más rápido y mayor dispersión de los solutos durante los periodos de infiltración, e influencia la tasa de mezcla en el sistema.

----- **Palabras clave:** Advección, enterramiento de minas, evaporación, flujo preferencial, infiltración, químicos relacionados con explosivos

Introduction

The transport and detection of organic compounds (TNT, DNT and related substances) derived from landmines sources are influenced by environmental, soil, and landmine source factors. These factors include: temperature, pressure, soil type (physical and chemical properties), water content, compaction, landmine flux, location, age and burial. Several studies have attempted to predict the effect of some of these factors, but few have studied the effect of the burial process on the transport of ERCs in soils. The transport of ERCs in soils occurs through advective (convective), dispersive, mass transfer, and reactive processes, which control their arrival time, mobility, and persistence in the environment. These processes are influenced by soil and environmental conditions such as: atmospheric pressure, wind,

relative humidity, temperature, infiltration, evapotranspiration, water content, sun light, soil type and its physical, chemical and biological properties [1, 2].

Preferential flow paths are associated to several factors, such as plant roots, shrinkage cracks, animal burrows, macropores, water repellency, air entrapment, small-scale variations in soil hydraulic properties, entrapped air behind the wetting front, and confined air ahead of the wetting front [3-5]. In large connected pores, fluids flow at higher velocities than the filtration velocities in the surrounding porous media. Limited studies have been conducted to evaluate the effect of burial of landmines on the transport of ERCs near soil-atmospheric surfaces under variable-saturated porous media [6, 7].

Materials and methods

Solute transport experiments were conducted in laboratory-scale soil columns subjected to infiltration, evaporation and reverse flow conditions. The soil column system permits 1D flow and 2D solute transport. It incorporates a uniform cylindrical stainless steel column (100 cm long and 19 cm ID) packed with a homogeneous sandy soil [8].

Experimental setup

The experimental setup consists of a solution-delivery and air-sweeping systems, vertically-placed sand columns, and vacuum and waste chambers (figure 1). The solution delivery system delivers the aqueous solution to the column and consists of solution reservoirs connected to liquid delivery pump. The air sweeping system delivers dry air across the soil surface to enhance evaporation.

The sand columns (figure 1) consist of a stainless steel (SS) tube (100 cm long by 19 cm ID) closed at both ends with SS caps. SS porous plates were placed at the bottom and top ends of the columns, respectively, to provide support for the porous media and maintain unsaturated water flux conditions at the bottom and atmospheric conditions at the top. Two soil columns were used, which contained sampling port clusters located at 19.5; 39.0; 58.5; and 78.0 cm from the bottom. Sampling clusters included a water pressure sampler, a liquid sampler, a gas pressure sampler, and a gas-phase sampler. The liquid and vapor samplers were used to measure the spatial and temporal concentration distribution of ERCs and other chemicals in the water and gas phases. Pressure samplers were used to monitor soil-water content and pressures and soil-gas pressure, and determine flow conditions. The samplers consist of stainless steel porous cups to selectively sample the water or the gas phases in the soil [9]. Experimental temperatures were achieved in the soil column by circulating water of at set temperature through copper coils.

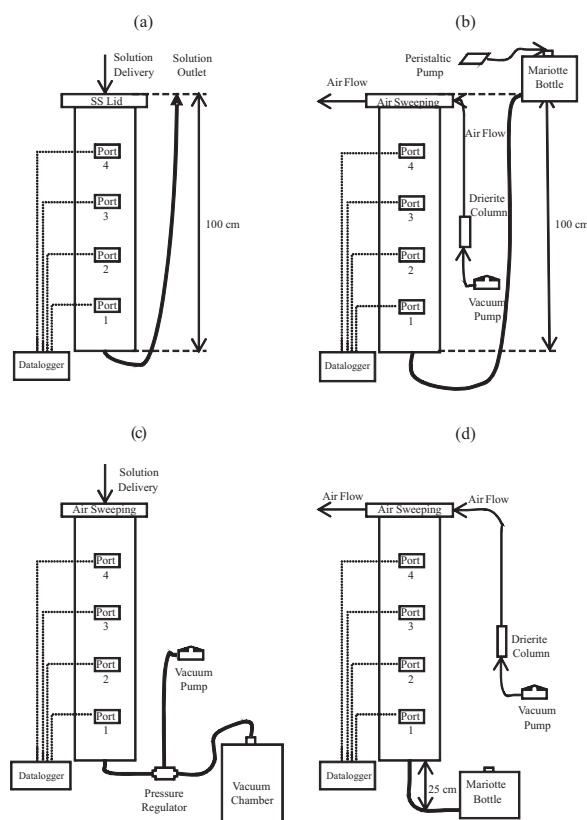


Figure 1 Experimental Setup for Saturated Conditions during Infiltration (a) and Evaporation (b) Events; and for Unsaturated Conditions during Infiltration (c) and Evaporation (d) Events

Soil properties

Transport experiments were conducted in stainless steel columns packed with beach sand from Isabela, Puerto Rico. This sand consists mainly of quartz and calcite, poorly graded, with a 2.83 g/cm^3 specific gravity and a $1.687 \text{ m}^2/\text{g}$ specific surface area [10]. Isabela sand is primarily composed of 92.6% sand sizes, and 7.4% of fines (silts and clays). The sand was packed in the stainless steel column following a procedure developed by [11] to achieve consistent and reproducible bulk densities and soil porosities. The sand was packed to a bulk density of 1.65 g/cm^3 and a media porosity of 41%. These values are within acceptable bulk density and porosity range for natural sandy soils [3, 12].

Transport experiments

Transport experiments involved introducing a TNT/DNT point source below the soil surface, and inducing infiltration and evaporation events, while monitoring chemical concentrations in the aqueous and gaseous phases. The transport experiments (table 1) involve burying a point source containing TNT and DNT crystals and allowing water to flow through the soil and the source under infiltration or evaporation conditions. A total of six (6) experiments were conducted under different water content, flow, and temperature conditions (table 1). TNT and DNT crystals were placed in a nylon bag (pore size $\sim 49 \mu\text{m}$), simulating a landmine point source. The source was buried at the center of the column, 13 cm from the soil surface (9 cm above Port 4).

Transport experiment started by initially imposing infiltration events, followed by evaporation events. Infiltration conditions were imposed by injecting a 20 mM NaCl tracer solution at the top of the column until the NaCl front reached the bottom of the column (Port 0), displacing an initial 4mM NaCl solution. Evaporation conditions were imposed after infiltration periods by discontinuing the delivery of the infiltrating solution, and passing dry air through the air-sweeping system on top of the column. Under saturated conditions, a constant head was maintained at the top of the column to replenish the evaporated water. Under unsaturated conditions, a constant tension head was maintained at the bottom of the column to replenish the evaporated water. The effect of 20 mM NaCl solution on the transport processes of ERCs is considered negligible [13].

Table 1 Description of experimental conditions

Experiment Number	Temperature (°C)	Degree of Saturation (%)	Flow Regime		
			Infiltration ⁽¹⁾		Evaporation
			Rate (cm/min)	Period (min)	Period (min)
1	25	100	0.007	3,150	84,270
2	25	75	0.071	1,004	74,536
3	25	45	0.007	7,080	44,360
4 ⁽²⁾	35	100	0.007	27,300	99,740
5	25	60	0.035	7,320	64,880
6	35	60	0.035	7,380	64,880

⁽¹⁾ Infiltration Rate (cm/min) = Q/A , where $A = 283,4 \text{ cm}^2$

⁽²⁾ Experiment 4 consisted of 2 saturated infiltration/evaporation cycles

Aqueous and vapor samples were collected temporally and spatially during the experiments. Aqueous samples were withdrawn through the liquid sampling ports using a manual syringe. Vapor samples were obtained by introducing a Polydimethylsiloxane/divinylbenzene Solid Phase Micro Extraction (SPME) fiber (65 μm film coating from Supelco) supported in a fiber holder assembly into a septum nut fitting

located in the vapor sampler. The SPME fiber was introduced into the sampler and allowed to sample (sorb) vapor for a period of 4 minutes. After sampling, the fiber was desorbed in a Gas Chromatography (GC) for analysis. The concentration was plotted vs. time to establish breakthrough curve (BTC) at each sampling point. The BTC was then analyzed using moments analysis and numerical models.

Chemical analysis

Spatial and temporal concentrations of NaCl, TNT, and DNT in the soil water and air (only ERCs vapors) phases were estimated by analyzing water and vapor samples taken from samplers and outlet ports in the soil column system. NaCl concentrations were analyzed using conductivity detectors, whereas ERC solutes and vapors were analyzed using gas chromatography techniques.

TNT and DNT concentrations were analyzed using liquid-liquid extraction, which involves the use of isoamyl acetate (1:2 sample:solvent ratio) as the extractions solvent. Once extracted, the ERC in the extract was analyzed in a GC equipped

with an Electron Capture Detector (ECD) and a Thermionic Specific Detector (TSD). Vapors sampled with SPME were analyzed by inserting the SPME fiber into the sampler for 4 minutes [14].

Data analysis

The transport experiments generated spatial and temporal pressure and concentration data. Spatial and temporal concentration breakthroughs, also known as breakthrough curves (BTCs) were analyzed comparatively and analytically to determine transport behavior of solutes and ERCs under the imposed conditions. The analytical assessments are presented in table 2.

Table 2 Analytical assessments for data analysis

Determination	Mathematical model	Reference	Comments
Temporal concentration distribution	$M_n = \int_0^{\infty} t^n C(z, t) dt \quad (1)$	[16]	Solution using the method of moments (MOM)
Mean arrival time of the center of NaCl mass (μ)	$\mu = \frac{M_I^I}{M_0^I} - \frac{M_I^I}{M_0^I} \quad (2)$	[16]	First normalized absolute moment of the input pulse and the effluent concentration
Effective water content	$\theta_e = \frac{Q}{A \cdot v} \quad (3)$	[16]	Estimated from the Darcy flux divided by the moment-derived pore water velocity
Numerical solution of Richards' equation.	Mathematical model HYDRUS 2D	[15]	Analysis for saturated - unsaturated water flow and convection-dispersion equation for heat and solute transport
Solute transport	$D = \varepsilon \cdot v + D^* \quad (4)$	[15]	Convective-dispersive transport in the liquid phase, as well as diffusion in the gaseous phase
Simulation of NaCl infiltration	Non equilibrium, Mobile-Immobile Model (MIM)	[8]	Analysis of preferential flow in column

Where for equation:

- (1) C is the solute concentration, z is the spatial coordinate and t is the time.
- (2) I and II superscripts refer to the moments of the input and output signals, respectively.
- (3) Pore water velocity ($v = L/\mu$), L, is column length, θ_e is an effective water content.
- (4) D, is dispersion coefficient, ε is the dispersivity and D^* is the effective diffusion coefficient.

Results and Discussion

NaCl BTCs were analyzed using the method of moments (MOM) on temporal concentration distributions. The zeroth and first moments were determined for the displacement of background solution (termed frontal elution, table 3). Frontal elution moments were estimated as indicated in equation 5:

$$M_n = \int_{t=0}^{t=t^*} \left(1 - \frac{C}{C_0}\right) t^n dt \quad (5)$$

Soil and transport parameters obtained during the analysis of moments for the NaCl BTCs achieved through the experimental period are presented in table 3, showing high variability in the pore water velocities and effective water content with depth. Although the sandy soil used in these experiments is relatively homogeneous, water content estimates and NaCl temporal distributions indicate the existence of hydraulic heterogeneities and preferential flow paths in saturated and unsaturated media during infiltration events. Generally, the results indicate that pore-water velocities for infiltrating conditions tend to decrease with depth (table 3). For constant flow conditions, as those imposed in the experiments, decreasing velocities reflect higher effective water contents with depth. For saturated conditions, saturated water contents (i.e., porosity) is not expected to vary with depth for homogeneous media, variations in the estimated effective water contents are attributed to differences in sampling volumes of the pore ensemble. This variability suggests preferential flow paths resulting from burial disturbances. In the presence of preferential flow paths, solutes are preferentially transported through a smaller pore volume, and may not participate over the entire column area near the surface. As the mixing process continues and the burial effects dissipate, solutes are able to sample a greater pore volume, as reflected by a greater effective water content with depth. These results suggest that disturbances near the buried source result in hydraulic heterogeneities and preferential flow near the source, which also influences their transport away from the source.

In unsaturated media, preferential flow is further accentuated by variable water contents with depth, resulting from flow and boundary conditions. Water contents determined from soil-water pressures and soil-water characteristic curves [8] show variations along the depth of the column (table 3). The results show that the estimated effective water contents are mostly lower than measured values. The percent difference between measured and estimated values is higher (~70%) for lower water contents, and averages about 60% among all unsaturated experiments. This is indicative of a low percentage of pores being sampled in the systems by the path of solutes, and thus, preferential flow. The preferential flow path pattern near the surface is stronger as the soil dries up. NaCl BTCs normalized to distance (using pore volumes = tL/v , v estimated from the MOM) in port 4 during infiltration process shows earlier initial arrival and more tailing as water content decreases (figure 2).

Generally, effective water contents during infiltration periods in unsaturated flow tend to be lower at higher temperatures (35°C), suggesting smaller sampling volumes and higher preferential flow (table 3). Greater differences between measured and estimated water contents (table 3) suggest greater influence of preferential flow paths at higher temperatures. This is attributed to the lower water contents attained at higher temperatures and greater water content and flow heterogeneities.

Preferential flow during infiltration processes is also supported by the results obtained from a moment analysis and HYDRUS 2D numerical model, which simulated homogeneous hydraulic conditions. Comparison between the experimental BTCs and the results predicted by the model show significant differences. Although differences are expected between simulated and measured temporal distributions because of the simplifying assumptions used in the model, the results support faster movement near the soil surface and slower near the column outlet relative to homogeneous systems not influenced by preferential flow (table 4).

Table 3 Parameters Obtained from NaCl BTCs using the MOM during Infiltration Process

<i>Experiment</i>	<i>Parameter</i>	<i>Front Elution</i>				
		<i>Port 4</i>	<i>Port 3</i>	<i>Port 2</i>	<i>Port 1</i>	<i>Port 0</i>
1	Mean Arrival Time (μ , min)	336.57	894.2	1,587.27	2,332.82	4,331.19
	Pore Water Velocity (v , cm/min)	0.07	0.05	0.04	0.03	0.02
	Effective Water Content (θ_e , %)	10.79	15.2	18.36	20.44	30.55
	Measure Water Contents (%)					
2	Mean Arrival Time (μ , min)	32.38	67.43	100.8	112.56	425.24
	Pore Water Velocity (v , cm/min)	0.68	0.62	0.61	0.72	0.24
	Effective Water Content (θ_e , %)	10.38	11.46	11.66	9.86	30.00
	Measure Water Contents (%)	26.0	23.5	25.0	25.0	ND
3	Mean Arrival Time (μ , min)	171.03	420.17	550.87	676.57	1,208.26
	Pore Water Velocity (v , cm/min)	0.13	0.1	0.11	0.12	0.08
	Effective Water Content (θ_e , %)	5.48	7.14	6.37	5.93	8.52
	Measure Water Contents (%)	20.0	23.0	21.0	18.0	ND
4	Mean Arrival Time (μ , min)	680.66	1,177.7	1,908.08	2,915.48	4,235.78
	Pore Water Velocity (v , cm/min)	0.03	0.04	0.03	0.03	0.02
	Effective Water Content (θ_e , %)	11.19	10.26	11.31	13.09	15.31
	Measure Water Contents (%)					
5	Mean Arrival Time (μ , min)	239.76	189.63	188.39	222.06	325.48
	Pore Water Velocity (v , cm/min)	0.09	0.22	0.32	0.36	0.31
	Effective Water Content (θ_e , %)	38.44	16.12	10.89	9.73	11.48
	Measure Water Contents (%)	25.0	24.0	24.5	21.0	ND
6	Mean Arrival Time (μ , min)	42.4	89.31	166.23	214.66	367.86
	Pore Water Velocity (v , cm/min)	0.52	0.46	0.37	0.38	0.27
	Effective Water Content (θ_e , %)	6.80	7.59	9.61	9.41	12.97
	Measure Water Contents (%)	22.0	20.0	21.0	31.0	ND

Generally greater dispersion is observed with solute traveling distance (i.e., with depth for infiltration conditions and upward distance in evaporation conditions). This is attributed to greater velocity variations caused by preferential flow, depth-dependent variable flow, and dispersive (mechanical and diffusive) mechanisms. Greater apparent dispersion for

evaporation conditions result from additional velocity variation caused by flow reversal processes. Dispersivity estimates from HYDRUS 2D [8] suggests higher dispersivity values than previously reported for homogeneous sand. The higher-than-expected values suggest preferential flow processes and hydraulic heterogeneity (table 4).

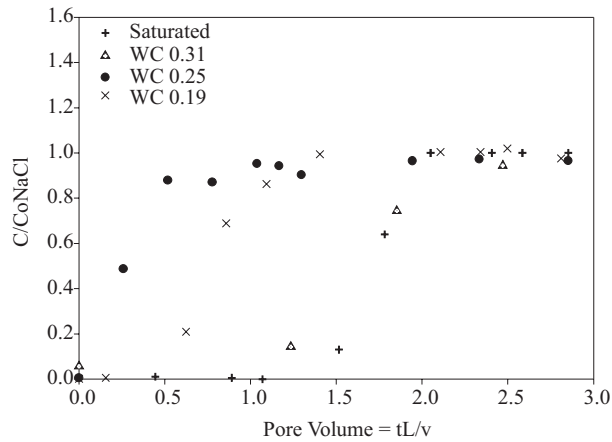


Figure 2 NaCl BTC Arrival in Port 4 during Infiltration Process under Different Water Contents at 25°C

Table 4 Estimated Transport Parameters for NaCl during Infiltration Process

Experiment	MOM	MIM using HYDRUS			ε (cm)
	v (cm/min)	v (cm/min)	DL (cm ² /min)	θ_{imw}	
1	0.05	0.01	0.03	0.1	3.555
2	0.65	0.06	0.04	0.1	0.697
3	0.11	0.03	0.09	0.1	2.871
4	0.03	0.01	0.04	0.1	6.064
5	0.25	0.04	0.13	0.1	3.232
6	0.43	0.04	0.06	0.1	1.594

The temporal distributions of TNT and DNT in water through the column (figures 3 through 5) show high concentration variability. This variability is mostly attributed to spatial and temporal variations in transport processes. For saturated conditions (figures 3a and 4a) TNT and DNT during infiltration events are initially detected in the upper most port (port 4). TNT and DNT concentrations at this location, which is closest to the DNT/TNT source (~10 cm from source), initially increase with time, reaching nearly constant concentrations of about 12 and 14 mg/L, respectively. Solute breakthroughs at deeper locations are generally eluted in an order related to the depth location, but at lower concentrations than in the upper-most

The dispersivity coefficient (ε) was estimated from MIM-generated dispersion coefficient (D_L) and velocities. The immobile water fraction (θ_{imw}) was assumed as 0.1 considering the literature reviewed for sandy soils [17]. Higher than expected dispersivity values were calculated for saturated values. Previous studies have reported dispersivities between 0.03 and 0.04 cm [3, 16]. Dispersivity estimates at 25°C suggest slight decrease with decreasing water contents. This suggests greater hydraulic heterogeneities at higher water contents.

port. Concentrations in port 3 are generally the most variable, suggesting an erratic movement of flow in the granular soil. At later infiltration times TNT and DNT solute concentrations in the lower-most port (port 1) tend to be higher than those measured in higher ports (port 3 and port 2). The general order of elution (i.e., earlier for closer-downstream locations) indicate that TNT and DNT solutes are moving with infiltrating water. The lower-than-solubility concentrations indicate that the dissolution processes of TNT and DNT is rate limited. The higher DNT solute concentrations (figures 3 through 5) are attributed to the higher dissolution capacity of DNT than TNT. Similar behavior in concentration variations of TNT and

DNT indicate that both solutes are influenced by similar transport processes. The initial presence of TNT and DNT varied as a function of time for the different sampling ports, detecting at approximately 500 min near the closest point from explosive source (port 4), at 1,500 min in port 3, 2,600 minutes in port 2, and at 3,700 minutes in port 1, which corresponds to the most distant point from the source. This result indicate that TNT and DNT move in the soil at a rate ranging between 0.017 and 0.018 cm/min, which is slower than the velocities estimated for the NaCl tracer and suggest solute retardation caused by sorption.

Lower solute concentrations at lower depth (i.e., greater transport distance) are attributed to preferential flow and incomplete mixing of the solute during initial transport distance after dissolution source. Because the upper-most sampling port is directly below the ERC source, solute at this location do not have enough mixing time and concentrations are high. As solutes continue to move downward they mix with solute-free water and concentrations are lowered. Higher concentrations at latter infiltration times in the lowest port suggest solute accumulation near the outflow boundary. This may also result from greater mass arrival through time as preferential flow paths converge toward the outflow boundary (figure 5).

During evaporation processes, unsaturated conditions (figures 3b and 4b), TNT and DNT

solute concentrations tend to decrease initially in the upper ports. For the lower ports, the concentrations increase initially after the onset of the evaporation period and then decrease. Solute concentrations in all ports increase significantly after a long evaporation period (>50.000 minutes). TNT and DNT concentrations during evaporation periods in unsaturated conditions tend to decrease with time to an asymptotic value (figures 3b and 4b). Decreasing concentrations in the lower-most ports are also associated with the upward movement of a solute-free solution as evaporation takes place. Significant increase in concentrations after long evaporation periods is attributed to solute accumulation caused by water evaporation. Temporally, this significant increase is observed initially at the upper-most port and later at deeper locations.

TNT and DNT concentrations in unsaturated infiltration (figure 5) indicate lower solute concentrations as water content decreases. The lower concentrations are attributed to rate-limited dissolution and increasing preferential flow as water content decreases. The greater preferential flow results in lower water flux through the TNT/DNT source causing lower dissolution flux. Because flow is only concentrated in preferential flow paths, there is greater velocities in those flow paths (than if the flow was evenly distributed). Greater velocities (table 3) result in lower concentrations if the dissolution process is rate-limited (figures 3 through 5).

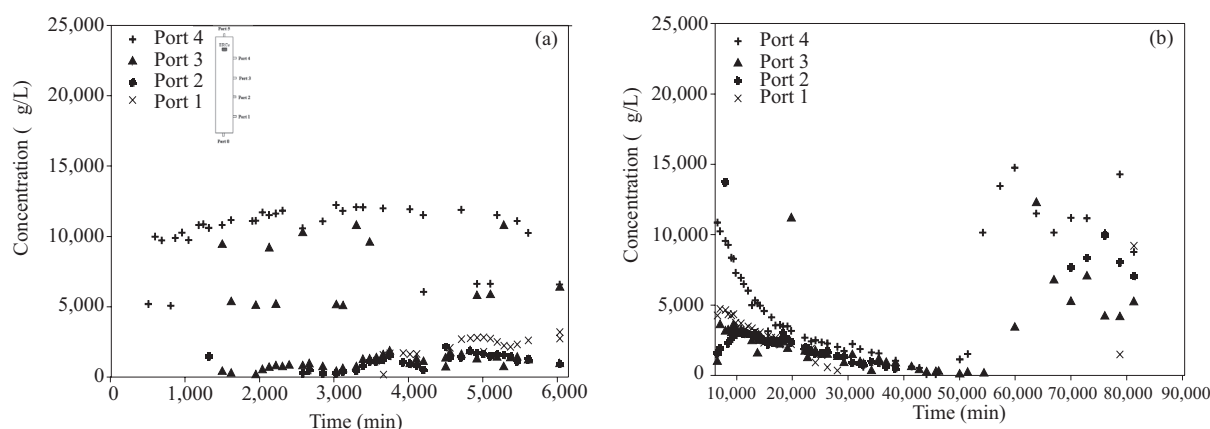


Figure 3 TNT_w BTC during Infiltration (a) and Evaporation (b) Processes under Saturated Conditions at 25°C (Exp 1)

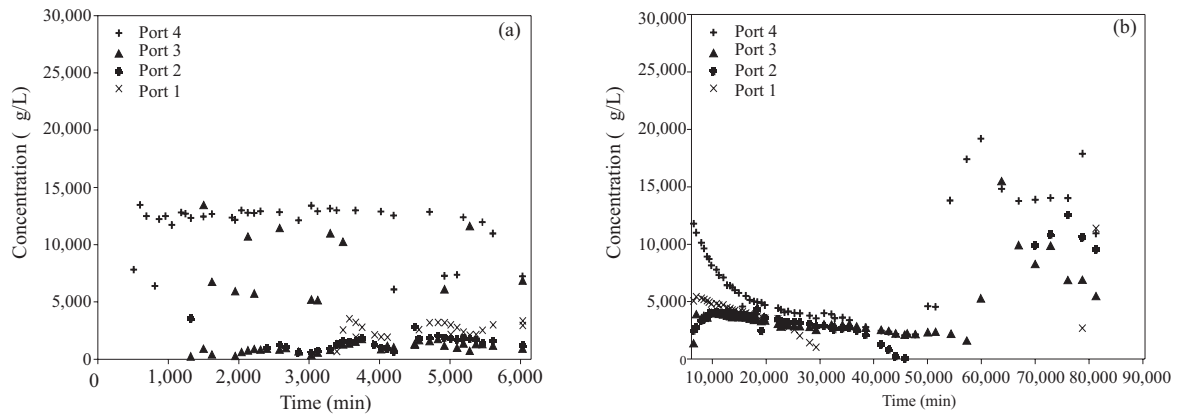


Figure 4 DNT_w BTC during Infiltration (a) and Evaporation (b) Processes under Saturated Conditions at 25°C (Exp 1)

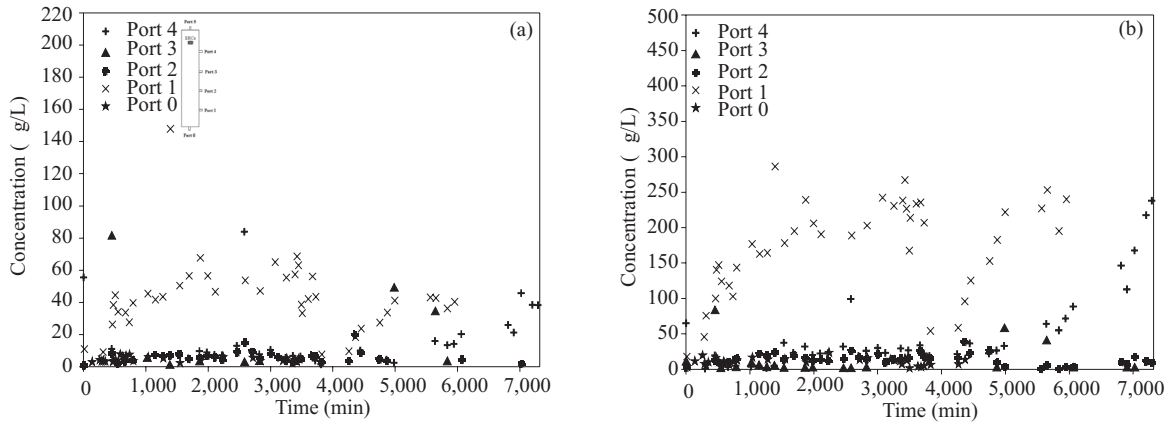


Figure 5 TNT_w (a) and DNT_w (b) BTCs during Infiltration Process under 60% of Saturation at 25°C (Exp 5)

Higher vapor phase concentrations at higher temperatures result from higher vapor pressures of TNT and DNT. Generally, lower variability is

observed in vapor concentration distribution at higher temperatures for saturated (figure 6) and unsaturated conditions (figure 7).

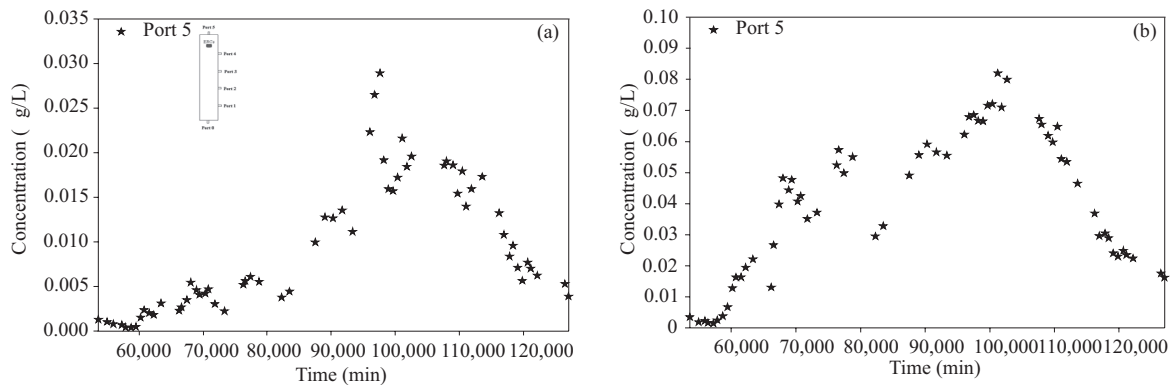


Figure 6 TNT_g (a) and DNT_g (b) BTCs in the Surface of the Soil during Evaporation Process in the Second Stage of the Experiment under Saturated Conditions at 35°C (Exp 4)

The lower variability at saturation is caused by homogeneous volatilization through the air-water interface phase at the surface of the soil. The greater volatilization variability caused by irregular interfacial areas in unsaturated flow, is however masked at higher temperature because of the greater volatilization rates.

The vapor concentrations of TNT and DNT decrease significantly after a long evaporation period, for both saturated and unsaturated conditions. The decrease is attributed to vapor flux losses to the atmosphere at greater rates that volatilization sources from soil-water (figures 6 and 7).

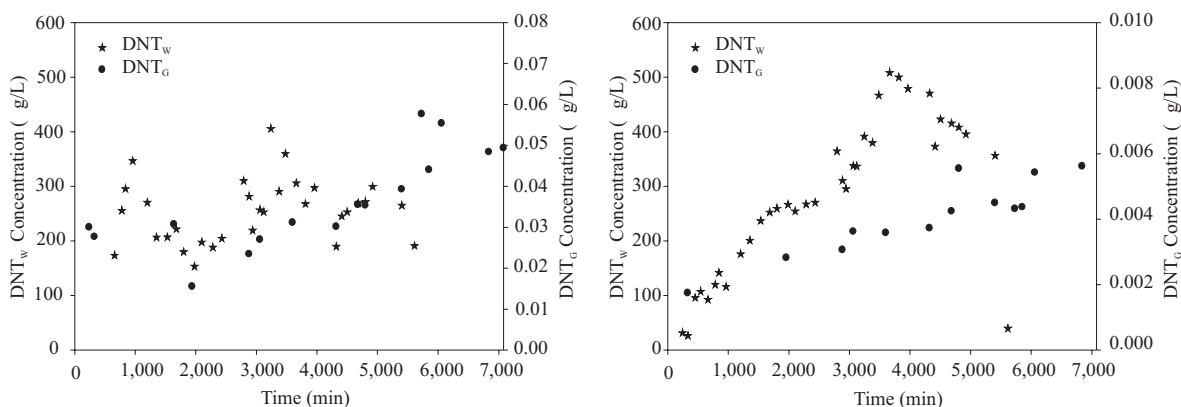


Figure 7 DNT_w vs. DNT_g during Infiltration Process for Port 4 (a) and Port 3 (b), under 60% of Saturation at 35°C (Exp 6)

Preferential flow and incomplete mixing of the TNT and DNT solutes near the source result in lower concentrations with depth. This also results in greater dispersion of the solutes, indicating greater expansion of the plume. Variable TNT and DNT aqueous concentration with time after infiltration periods indicate that their fate and transport is influenced by water redistribution, upward movement of solute-free water during evaporation, and solute accumulation caused by water evaporation at the soil surface. Generally, TNT and DNT solute concentration tend to decrease with time after water redistribution processes caused by drainage. The decrease is attributed to slow dissolution kinetics, and sorption, and volatilization losses. Although some degradation losses may be possible, there is no evidence of major degradation processes [8].

Conclusions

- Results from experimental data and numerical simulations indicate that water content and movement near TNT and DNT

buried sources is the most important factors affecting their transport in soils and near-atmospheric surfaces. Higher water contents enhance source dissolution and induces greater extension of the chemical plume. Disturbances of soil properties by burial of ERC sources are likely to result in hydraulic heterogeneities and preferential flow near the source. The transport of TNT and DNT in soils subjected to variable flow and water contents are influenced by dissolution (source-water), volatilization (water-air), and sorption (water-soil) mass transfer limitations. Greater dispersion was observed with solute traveling greater distance during both infiltration and evaporation periods due to greater velocity variations caused by preferential flow, depth-dependent variable flow, and dispersive (diffusion and mechanical) mechanisms. Research using 3D analysis is necessary to determine the influence of the burial on the transport of TNT and DNT considering that explosives are not expected to move just vertically but horizontally.

Acknowledgments

This research was supported by Army Research Office. DoD MURI Program. Grant No. DAAD 19-02-1-0257. The authors express their gratitude for financial, scientific and technical support provided DoD-ARO. Night Vision Laboratory and JUXOCO.

References

1. S. W. Webb, K. Pruess, J. Phelan, S. Finsterle. "Development of a Mechanistic Model for the Movement of Chemical Signatures from Buried Landmines/UXO". *Proceedings in Detection and Remediation Technologies for Mines and Minelike Targets IV. SPIE Defense and Security Symposium*. Vol. 3710. 1999. pp. 270-282.
2. S.W.Webb,J.M.Phelan. "Effect of Diurnal and Seasonal Weather Variations on the Chemical Signatures from Buried Landmines/UXO". *Proceedings in Detection and Remediation Technologies for Mines and Minelike Targets V. SPIE Defense and Security Symposium*. Vol. 4038. 2000. pp. 474-488.
3. C. W. Fetter. *Contaminant Hydrogeology*. Ed. Prentice Hall Inc. New Jersey. 1999. pp. 53-78, 200-204.
4. M. Ghodrati, W. A. Jury. "A Field Study Using Dyes to Characterize Preferential Flow of Water". *Soil Science Society of America Journal*. Vol. 54. 1990. pp. 1558-1563.
5. S. A. Hagrey, T. Schubert-Klempnauer, D. Wachsmuth, J. Michaelson, R. Meissner. "Preferential Flow: First Results of a Full-Scale Flow Model". *Geophysical Journal International*. Vol. 138. 2002. pp. 643-654.
6. D. Wildenschild, K. H. Jensen. "Laboratory Investigations of Effective Flow Behavior in Unsaturated Heterogeneous Sands". *Water Resources Research*. Vol. 35. 1999. pp. 17-28.
7. J. M. Phelan, S. W. Webb, M. Gozdzor, M. Cal, J. L. Barnett. "Effect of Soil Wetting and Drying on DNT Vapor Flux – Laboratory Data and T2TNT Model Comparisons". *Proceedings in Detection and Remediation Technologies for Mines and Minelike Targets VI. SPIE Defense and Security Symposium*. Vol. 4394. 2001. pp. 868-878.
8. J. P. Gutiérrez. *Effects of Flow Reversal on Two-Dimensional Transport of Explosive Chemicals in Soils*. Thesis. University of Puerto Rico. Puerto Rico. 2008. pp. 78-89, 107-112.
9. A. C. Padilla, I. Y. Padilla, I. Santiago. "Multiphase Extraction Sampling of Explosives in Unsaturated Soils". *Proceedings in Detection and Remediation Technologies for Mines and Minelike Targets XI. SPIE Defense and Security Symposium*. Orlando. FL. Vol. 6217. 62173C. 2006. pp. 1-11.
10. G. I. Molina, I. Padilla, M. Pando, D. Pérez. "Field Lysimeters for the Study of Fate and Transport of Explosive Chemical in Soils under Variable Environmental Conditions". *Proceedings in Detection and Remediation Technologies for Mines and Minelike Targets XI. SPIE Defense and Security Symposium*. Orlando. FL. 2006. Vol. 6217.62137A. pp. 1-12.
11. S. Rodríguez, I. Padilla, I. Santiago. "Development of a Multi-Scale Packing Methodology for Evaluating Fate and Transport Processes of Explosive-Related Chemicals in Soil Physical Models". *Proceedings in Detection and Remediation Technologies for Mines and Minelike Targets XI. SPIE Defense and Security Symposium*. Orlando. FL. 2006. Vol. 6217. 6217U. pp. 1-10.
12. J. M. Phelan, S. W. Webb. "Chemical Detection of Buried Landmines". *Mine Warfare Association. Proceeding of the 3rd International Symposium on Technology and the Mine Problem*. 1998. SAND-98-0576C CONF-980427. pp. 1-11.
13. J. M. Brannon, C. B. Price, P. S. Yost, C. Hayes, B. Porter. "Comparison of Environmental Fate and Transport Process Descriptors of Explosives in Saline and Freshwater Systems". *Marine Pollution Bulletin*. Vol. 50. 2005. pp. 247-251.
14. A. Torres, I. Padilla, S. Hwang. "Physical Modeling of 2,4-DNT Gaseous Diffusion through Unsaturated Soil". *Proceedings of SPIE. Detection and Remediation Technologies for Mines and Minelike Targets XII. SPIE Defense and Security Symposium*. Orlando. FL. 2007. Vol. 6553. 65531Q. pp. 1-12.
15. J. Šimůnek, M. Šejna, M. Th. van Genuchten. "The HYDRUS Software Package for Simulating the Two and Three Dimensional Movement of Water". *Heat, and Multiple Solutes in Variably-Saturated Media*. U.S. version 1.0. Salinity Laboratory. Riverside. California. 2006. pp. 203.
16. I. Y. Padilla, T. C. Jim Yeh, M. H. Conklin. "The Effect of Water Content on Solute Transport in Unsaturated Porous Media". *Water Resources Research*. Vol. 35. 1999. pp. 3303-3313.
17. Y. M. Oliver, K. R. J. Smettem. "Parameterisation of Physically Based Solute Transport Models in Sandy Soils". *Australian Journal of Soil Research*. Vol. 41. 2003. pp. 771-788.